1-2010

Molecular modulation of Schottky barrier height in metal-molecule-silicon diodes: Capacitance and simulation results

Adina Scott
Purdue University - Main Campus, scott26@purdue.edu

Chad Risko
Northwestern University

Nicholas Valley
Northwestern University

Mark A. Ratner
Northwestern University

David B. Janes
Purdue University, david.b.janes.1@purdue.edu

Molecular modulation of Schottky barrier height in metal-molecule-silicon diodes: Capacitance and simulation results

Adina Scott,[1,a)] Chad Risko,[2] Nicholas Valley,[2] Mark A. Ratner,[2] and David B. Janes[1]
[1]*School of Electrical and Computer Engineering, Birck Nanotechnology Center, Purdue University, West Lafayette, Indiana 47907, USA*
[2]*Department of Chemistry, Northwestern University, Evanston, Illinois 60208, USA*

(Received 8 August 2009; accepted 21 September 2009; published online 25 January 2010)

There is considerable current interest in using molecular materials to influence the surface potential of semiconductor devices for nanoelectronic and sensing applications. We present experimental capacitance-voltage results showing that systematic Schottky barrier height modulation can be achieved using dipolar molecular layers in gold-molecule-silicon devices. A computational methodology that combines quantum chemistry and traditional electrostatic calculations is used to explore various physical effects that can influence barrier heights in such systems. Nonidealities such as silicon surface states can influence both the potential profile within the device and the validity of the extracted barrier height. Our devices exhibit low surface state densities, but the magnitude of surface potential modulation is modest due to molecular depolarization from the gold contact. © *2010 American Institute of Physics*. [doi:10.1063/1.3251466]

I. INTRODUCTION

Integrating organic molecules with solid-state electronic devices is a topic of great current interest.[1–3] By combining the electronic properties of semiconductors with the chemical, biological, and molecular electronic versatility of organic materials, a variety of novel devices can be realized. This approach may enable significant advances in chemical and biological sensing, electronic devices, energy conversion, and a variety of other applications. Although well-developed theories exist to describe the physics of electronic devices and molecular materials independently, the electronic properties of hybrid devices are poorly understood. To describe such structures in a meaningful, physically realistic manner, theoretical and analytical techniques must be adapted to address their unique properties.

One class of hybrid device that has been extensively studied is the molecularly modified Schottky diode.[4–8] Such devices consist of a molecular layer bound to a moderately doped semiconductor with a metal contact. There is an offset between the metal work function and the semiconductor electron affinity, yielding a substantial Schottky barrier and a depletion region in the semiconductor at zero bias; these electrostatic properties result in devices exhibiting classic Schottky diodelike behavior.[9–11] In such devices, the molecular layer modulates electronic properties due both to molecular electronic effects and to it's electrostatic influence on the substrate.[12,13] It has been demonstrated that dipolar molecular layers deposited on semiconductor surfaces can modulate the surface potential in a controlled manner.[4] The influence of dipolar molecular layers on metal/molecule/semiconductor (MMS) device electrostatics is considerably more complicated. Metal-molecule interactions are often critically important in determining device behavior.[14] It has been found that both the magnitude and direction of Schottky barrier height modification can be influenced by such interactions.[14,15] In addition to changing the device electrostatics, the molecular layers can modify junction properties such as semiconductor surface state densities and distributions, which can in turn influence the measured device characteristics. In most studies, the devices are analyzed using standard experimental methods for relatively ideal Schottky-barrier diodes;[16,17] however additional physical insight can be gained from more detailed theoretical consideration of the junction properties.

In this study, we present complementary capacitance experiments and calculations to explore various physical processes that can occur in MMS devices. Gold/molecule/*n*-type silicon MMS diodes with a series of substituted aryl molecular layers were fabricated and capacitance-voltage (*CV*) measurements were performed. The devices were analyzed using standard methods for Schottky diodes. Calculations were developed to determine device electrostatics and resulting *CV* characteristics including molecular capacitive effects, molecular charge density, and Si surface states. Experimentally, it is found that the addition of a dipolar layer induces modest changes in the apparent Schottky barrier height. By comparing the experimental results and calculations, it is possible to determine the physical effects responsible for the observed modulation in device behavior. Silicon surface states, molecular capacitive effects, molecular charge density, and metal-molecule interactions are explored to determine their influence on experimentally determined Schottky barrier heights.

II. EXPERIMENTAL

MMS diodes, as shown schematically in Fig. 1, were fabricated. ⟨111⟩-orientation *n*-type (*P*-doped, $N_d=3\times10^{15}$ cm^{-3}) Si wafers were cleaned, hydrogen terminated, and functionalized with the substituted aryl molecular species shown in Fig. 1. Details of surface modification and

[a)]Electronic mail: scott26@purdue.edu.

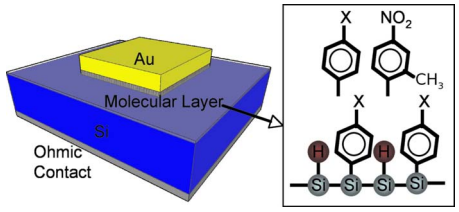

FIG. 1. (Color online) Schematic of MMS device used for capacitance measurements and molecular modifiers used in this experiment. X=Br (B-benz), $N(C_2H_5)_2$ (D-benz), OCH_3 (M-benz), NO_2 (N-benz), 2M 4N-benz.

characterization have been published previously.[18] The samples were metallized by deposition of 15 nm of gold using a "soft" evaporation procedure followed by 200 nm of gold applied using standard electron-beam vacuum evaporation.[9,10,19] Soft evaporation is performed in a standard thermal evaporator with the sample placed on a holder facing away from the gold source. After evacuation, the chamber is backfilled with argon to approximately 6 mTorr and the evaporation is performed at a rate of 0.1 Å/sec. Due to the process geometry, the gold atoms must scatter off the gas in the chamber before settling on the sample surface, thereby reducing the energy imparted to the sample and reducing the damage to the molecular layer.[20] Gold/hydrogen-terminated Si control samples (H-term) were fabricated by metallizing freshly etched Si. 50×50 μm^2, 100×100 μm^2, and 150×150 μm^2 device regions were defined by photolithography and wet etching of the gold. The photoresist was stripped using acetone and a large area back contact was applied with GaIn eutectic. Previous infrared and inelastic tunneling spectroscopic studies of similarly fabricated MMS devices indicate that these molecular layers are robust to the soft metallization and photolithography processing.[20]

MMS diodes were measured and analyzed using standard Schottky diode techniques. *CV* measurements were performed at room temperature in the dark using a Keithley 595 capacitance measurement system. The samples were mounted on steel sample pucks and placed on a vacuum chuck to achieve electrical contact to the back of the sample. The top metal electrode of the diode was contacted gently with a probe tip. A reverse bias of zero to 5 V was applied in 50 mV increments with a small-signal ac frequency of 100 kHz.

When a Schottky diode is reverse biased, a capacitance arises due to the depletion region in the semiconductor. The depletion capacitance can be modeled as a parallel-plate capacitor with a dielectric thickness equal to the depletion width given by

$$C = \frac{\varepsilon_0 \varepsilon_S A}{W_{\text{depl}}}, \tag{1}$$

where ε_0 and ε_S are the permittivity of free space and the semiconductor relative permittivity, respectively, W_{depl} is the depletion width, and A is the device area. The depletion width of an ideal Schottky diode is given by

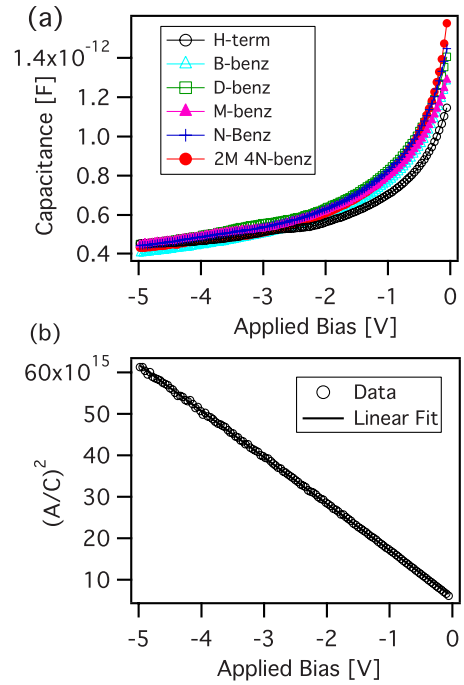

FIG. 2. (Color online) (a) Typical *CV* curves for gold/molecule/*n* Si devices and (b) typical $(A/C)^2$ vs V characteristic and linear fit of a representative MMS device.

$$W_{\text{depl}} = \sqrt{\frac{2\varepsilon_0 \varepsilon_S}{qN_d}(V_{\text{bi}} - V_{\text{appl}} - k_B T)}, \tag{2}$$

where N_d is the Si doping density, k_B is the Boltzmann constant, T is the temperature, and V_{bi} and V_{appl} are the built-in and applied voltages, respectively. Combining Eqs. (1) and (2), it is found that

$$\left(\frac{C}{A}\right) = \sqrt{-\frac{q\varepsilon_0 \varepsilon_S N_d}{2(V_{\text{bi}} - V_{\text{appl}} - k_B T)}}. \tag{3}$$

From Eq. (3), it is clear that the *CV* data can be plotted as $(A/C)^2$ versus V_{appl}. The plot is linear with a slope of

$$S = -\frac{2}{q\varepsilon_S \varepsilon_0 N_d} \tag{4}$$

and an intercept on the V_{appl}-axis of

$$V_i = V_{\text{bi}} - k_B T. \tag{5}$$

The barrier height is given by

$$\Phi_B = V_i + V_0 + k_B T, \tag{6}$$

$$V_0 = k_B T ln\left(\frac{N_c}{N_d}\right), \tag{7}$$

where $N_c = 3\times10^{19}$ cm^{-3} is the effective density of states in the Si conduction band, resulting in a V_0 of 0.293 eV.[21,22] Experimental and simulation results that verify the validity of this analysis procedure for the devices in this study will be presented.

Representative *CV* curves for various molecular species are shown in Fig. 2(a). A typical fit to the experimental data is shown in Fig. 2(b). For each sample type, at least 20

TABLE I. Doping densities and Schottky barrier heights for gold/molecule/*n* Si devices as determined from *CV* measurements.

Sample	Doping density (10^{15} cm^{-3})	Φ_B (eV)
H-term	5.62	0.852 ± 0.041
B-benz	8.37	0.780 ± 0.047
D-benz	6.21	0.901 ± 0.018
M-benz	6.98	0.868 ± 0.037
N-benz	6.95	0.786 ± 0.024
2M 4N-benz	5.81	0.762 ± 0.028

TABLE II. Calculated dipole moments (Debye) perpendicular to the Si surface for isolated molecular species used in this study assuming that the molecules orient perpendicular to the surface.

Molecule	Dipole (D)
Amino-benz	−1.96
D-benz	−2.39
M-benz	−0.53
B-benz	1.96
N-benz	4.56
2M 4N-benz	4.8

devices were measured. A small number of devices exhibited high leakage currents and the depletion capacitance could not be accurately determined. The yield of devices for which the capacitance could be measured ranged from 85%–100% for the samples in this study. The devices were analyzed using the methods outlined above; the barrier heights and doping densities extracted from these measurements are given in Table I. The doping densities extracted from the *CV* measurement are in reasonable agreement with the nominal doping density of the wafers.

III. SIMULATION

Well-known techniques exist to calculate charge distributions within isolated molecules and for ideal metal/semiconductor devices. Obtaining solutions for MMS electrostatics requires simultaneous consideration of molecular charge, semiconductor depletion, and surface-state effects. The overall *CV* relationship for a MMS structure can be calculated by solving Poisson's equation considering the charges in the molecular layer, interface states at the semiconductor surface, and bulk charge within the semiconductor depletion region. This section describes an approach that considers the molecular layer as a dielectric layer with charge sheets corresponding to Mulliken charges for the various atomic layers within a monolayer of the molecule.

As a first-order approximation, a molecular layer can be considered a thin dielectric layer between the metal and the Si surface. For MMS structures, the molecular layer contributes a molecular capacitance in series with the depletion capacitance given by

$$\frac{C_{\mathrm{mol}}}{A} = \frac{\varepsilon_0 \varepsilon_{\mathrm{mol}}}{t_{\mathrm{mol}}}, \tag{8}$$

where $\varepsilon_{\mathrm{mol}}$ is the relative permittivity of the molecular layer and t_{mol} is the molecular layer thickness. In the devices in this study, the molecular thickness is on the order of 1 nm, whereas the Si depletion width for modest reverse bias is more than three orders of magnitude larger. This leads to a situation where C_{mol} induces negligible changes in the Si surface potential (<10 mV). Since the junction capacitance is dominated by the Si depletion region, the molecular capacitance can be neglected while performing standard Schottky diode analysis without introducing a significant error.

Density functional theory (DFT) calculations were performed to determine the electronic structure of the molecules used in this study. The DFT calculations were carried out using the B3LYP functionals, where Becke's three-parameter hybrid exchange functional[23,24] is combined with the Lee–Yang–Parr correlation functional[25] and a 6-31G** split valence plus double polarization basis set for all nongold atoms; the SBKJC small-core, effective core potential was used for gold in order to take into account relativistic effects. All calculations were carried out with QCHEM (version 2.0) software suite.[26] Geometry optimizations were performed on the isolated molecular modifiers to determine the electronic structure and molecular dipole moments given in Table II; properties for amino-benzene (NH_2-*ph*) were calculated to assist with the interpretation of N-benz and 2M 4N-benz devices. Calculated molecular dipole moments are typically used as a basis for comparison in order to relate trends in device electrostatics to molecular headgroup electronegativity. This approach is often used because qualitative trends in MMS Schottky barrier heights correlate with the dipole moments of the isolated molecular modifiers, which can be calculated readily.[4,5,13]

The experimentally determined barrier heights are plotted as a function of calculated isolated molecule dipole in Fig. 3. It has been shown previously that the NO_2 substituent in the nitro-containing molecules can reduce to NH_x species, which have a very different molecular dipole moment.[18] The relative amounts of nitro-terminated and amine-terminated molecules in the layers were determined from the x-ray photoemission spectroscopy data. An equivalent molecular layer dipole was found by taking a weighted average of calculated dipoles for NO_2 and NH_2-substituted benzene. The molecular devices show small, systematic changes in measured

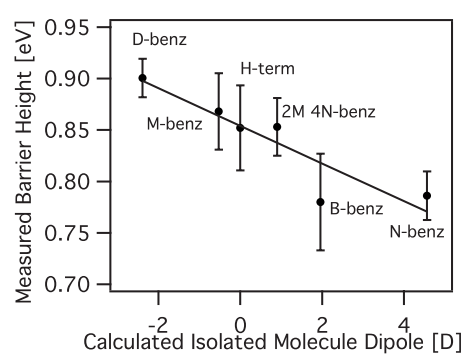

FIG. 3. Measured Schottky barrier height as a function of isolated molecule dipole moment for a series of MMS diodes.

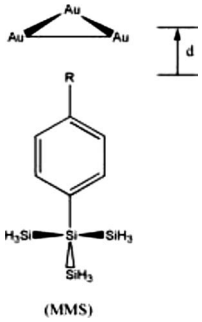

FIG. 4. Schematic of structure used to calculate MMS molecular-electronic properties. d is the spacing between the topmost heavy atom on the molecule and the gold cluster.

Schottky barrier height as a function of the dipole moment of the isolated molecular modifier. From a linear fit to the data set in Fig. 3, it is found that

$$\Phi_B = 0.854 - 0.0183 \times p[\mathrm{eV}], \tag{9}$$

where p is the calculated isolated molecular dipole in Debye (D).

Although qualitative trends in measured barrier heights can be explained in terms of relative isolated molecule dipoles, more quantitative models require the consideration of molecular properties as bonded to the contacts. Prior experiments suggest that the presence of a metal overlayer reduces molecular control over semiconductor surface potential.[15] Extended molecule simulations were performed with small silicon (Si_4H_9) and gold (Au_3) clusters to approximate contact effects. Geometry optimization of the as-grafted molecular layers on a small Si cluster was performed. Because the interaction between the molecule and the gold overlayer is not well defined, the gold cluster was placed above the molecular headgroup, as shown schematically in Fig. 4. Self-consistent field calculations were carried out at molecular headgroup to gold cluster distances of 2–3 Å to investigate geometric effects. The resulting molecular charge distributions were used to investigate electrostatic effects in MMS devices.

The Mulliken charge distributions from the DFT calculations were used to determine the expected potential profiles within the molecules. In this study, the molecules are assumed to be oriented normal to the Si surface and the packing density is assumed to be the ideal value of every other site on the Si surface (3.9×10^{14} mol/cm^2).[27] Different substituent chemistry will lead to some variation in molecular layer packing density, partial multilayer formation, and molecular orientation for various molecular layers; however, these effects are modest and will not be considered in this analysis.[18] Under these assumptions, the molecular layer charge distribution Q_{mol} can be expressed as a series of sheet charges

$$Q_{\mathrm{mol}} = \sum_i q_i N_{\mathrm{mol}} \delta(x_i), \tag{10}$$

where q_i is the equivalent electronic charge on a given atom, N_{mol} is the density of molecules on the surface, and x_i is the distance of the atom from the Si surface. A one-dimensional

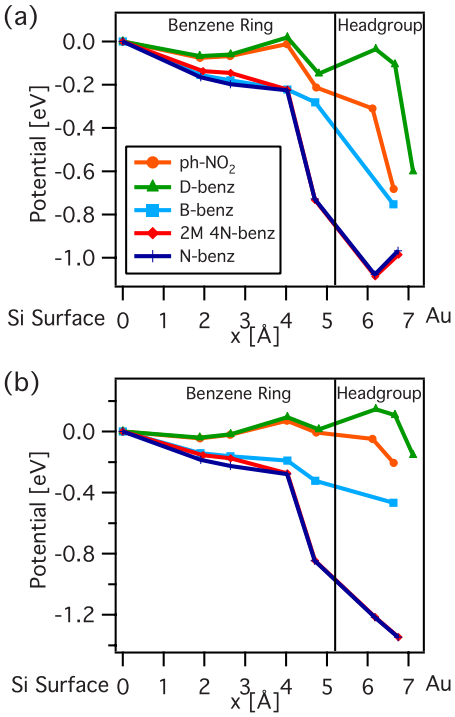

FIG. 5. (Color online) Calculated potential profiles across molecule for (a) $d=2$ Å molecule/gold spacing and (b) $d=3$ Å molecule/gold spacing. The legend in (a) is applicable to both plots.

Poisson solution was then found for the potential profile corresponding to the molecular layer charge density assuming a relative dielectric constant of 2.2 within the molecular layer. The resulting potential profiles are shown in Fig. 5. It is interesting to note that the headgroup electronegativity appears to have only a modest effect on the charge distribution in the phenyl ring with the exception of the topmost carbon atom. When the Au-molecule distance is 3 Å ($d=3$), there is a large variation in potential across the molecule [Potential($x=7$)−Potential($x=0$)] for the different molecular species. This is similar to the dipoles of the as-grafted or isolated molecules. On the other hand, when the Au-molecule distance is reduced to 2 Å ($d=2$), there is significantly less modulation in potential over the series of molecules because the gold electrostatically screens the molecular dipole. The calculated potential drop across the isolated molecule changes systematically with the isolated molecule dipole, as shown in Fig. 6. From a linear fit to the data it is found that

$$\Delta\Phi_B = -0.0481 \times p[\mathrm{eV}] \quad d_{\mathrm{Au}} = 2 \text{ Å},$$

$$\Delta\Phi_B = -0.1649 \times p[\mathrm{eV}] \quad d_{\mathrm{Au}} = 3 \text{ Å}. \tag{11}$$

This result indicates that molecular dipoles can induce changes in Si surface potential on the order of hundreds of meV; however the effect is very sensitive to the details of contact geometry due to screening effects.

This approximate molecular layer charge density can be incorporated into the insulating layer of a metal/insulator/Si diode and the electrostatics can be determined by a simple Poisson solution, as shown schematically in Fig. 7(a). In this method, the molecular charge density is fixed; however the

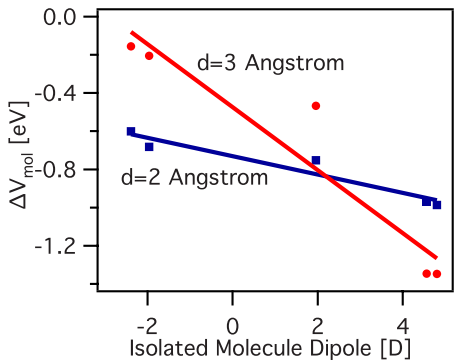

FIG. 6. (Color online) Calculated potential drop across molecule as a function of isolated molecule dipole.

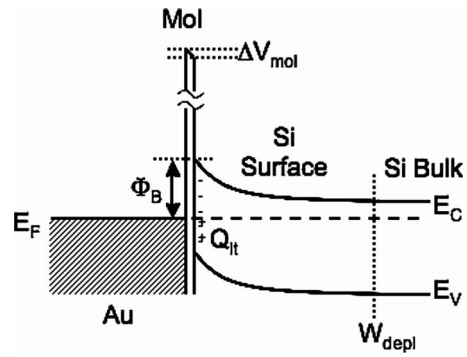

FIG. 8. Band diagram of MMS device. The actual barrier height (Φ_B) differs from the built-in potential because of the change in potential across the molecular layer (ΔV_{mol}) due to molecular capacitive effects and molecular dipole effects and the change in potential across the first few atomic layers at the Si surface due to interface charge (Q_{it}).

Si depletion width is allowed to adjust self-consistently to solve for the charge distribution within the Si and the potential profile within the device, as described in Fig. 7(b). Since the electric fields within the molecular layer are much larger then those in the Si due to the high degree of charge localization within the molecules, the potential profile across the molecule is not greatly affected by the inclusion of the Si electrode in the Poisson calculation. Quantitatively correct solutions will require calculation on an extended system to capture collective effects for large numbers of molecules.[28–31] Moreover, the Mulliken charge distributions must be adjusted based on the local built-in and applied electric fields to capture molecular polarization effects; however our simple approach provides qualitative information that can be used to explain experimentally observed trends.

Additional simulations were performed to estimate the influence of various effects on measured device characteristics. Surface state effects were included by adding an interface trap charge Q_{it} as a voltage-variable sheet charge at the Si/molecule interface. The Si is assumed to have a density of trap states D_{it}, uniformly distributed in energy throughout the Si bandgap. Based on prior experimental and theoretical studies of metal/Si Schottky diodes, a charge neutrality level of 0.55 eV relative to the Si valence band is assumed.[22] The interface trap charge is determined by self-consistently solving for the charge density and potential profile within the device using the algorithm in Fig. 7(b). Q_{mol} is obtained from the DFT calculations of the Mulliken charge and is kept fixed. Q_{it} and W_{depl} are adjusted to self-consistently solve for the charge distribution and device electrostatics. The "actual" Schottky barrier within the device can be found from the resulting potential profile at zero applied bias by taking the difference between the Si surface potential and the metal Fermi energy, as shown in the band diagram in Fig. 8.

The full *CV* characteristics were found by performing the Poisson calculation at various applied bias points. At each bias point, the device electrostatics were calculated by self-consistently solving for the charge distribution and potential profile within the junction as outlined above. The *CV* curves were calculated by considering that

$$C = \frac{dQ}{dV}. \tag{12}$$

The terminal capacitance is

$$C_{meas} = \frac{dQ_{depl}}{dV} + \frac{dQ_{it}}{dV}. \tag{13}$$

Typical as-simulated *CV* curves with a Si doping density of 10^{15} cm^{-3} are shown in Fig. 9. The discreteness in the curves is due to the simulation grid. The presence of large charge densities varying over small distances caused such apparent discretization of the charge. A more sophisticated mesh can be used to improve the resolution. Equation (13)

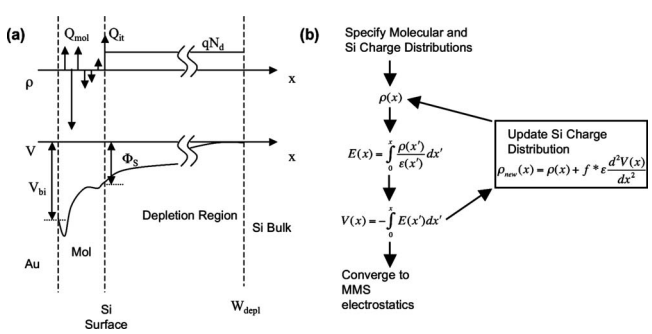

FIG. 7. (a) Schematic of the charge distribution (ρ) and resulting potential profile (V) in a MMS device and (b) flowchart illustrating self-consistent Poisson solution methodology for MMS diodes. $E(x)$ is the electric field, $\varepsilon(x)$ is the permittivity, and $0<f<1$ is a weighting factor that is used for convergence purposes. The molecular charge density, interface trap charge, and semiconductor depletion charge can all be incorporated in $\rho(x)$.

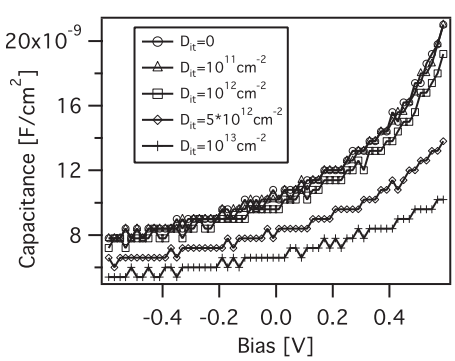

FIG. 9. Representative simulated *CV* curves for MMS devices. The discreteness in the curves is due to the simulation grid and the presence of large charge densities varying over small distances.

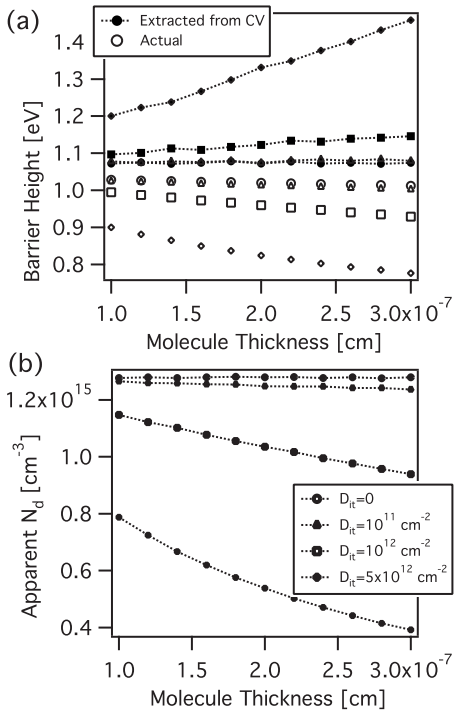

FIG. 10. Effect of interface state density on apparent (a) barrier height and (b) doping density. The legend in (b) applies to both graphs.

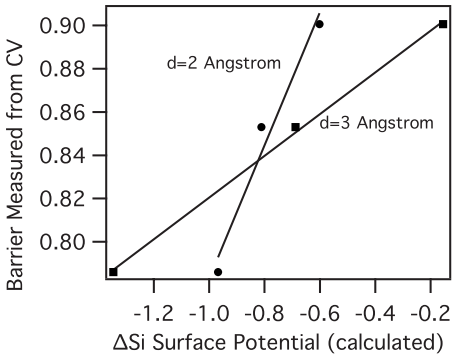

FIG. 11. Comparison of barrier height as measured by *CV* and calculated changes in Si surface potential.

represents the quasistatic terminal capacitance. As long as the dc sweep of the capacitance measurement is sufficiently slow that the depletion width and interface charge can respond, the physical insights from the quasistatic case can be applied to the ac capacitance measurement.

From the simulated *CV* curves, the apparent barrier heights and doping densities were determined using the same procedure as for the experimentally measured curves. Because an accurate potential profile is determined from the simulation, the actual and extracted barrier heights can be compared, illustrating physical processes that affect the validity of extracted device parameters. *CV* curves of MMS devices with varying molecular capacitive properties and Si surface state densities were simulated to determine the influence of these parameters on the extracted Schottky barrier height. Actual values for the barrier height and doping density may have some error due to the simulation grid; however trends can be used to understand physical processes that can affect the validity of parameters determined using the *CV* measurement.

Barrier heights and doping densities as determined from calculated *CV* curves for devices including interface trap effects and molecular capacitance are shown in Fig. 10. Since the molecular layer thickness, defined as the distance from the Si surface to the topmost heavy atom of the molecule, is much smaller than W_{depl} in reverse bias, the molecular capacitance does not induce a measurable change in Φ_B. In the presence of Si surface states, the actual Schottky barrier decreases as the thickness of the molecular layer increases [open symbols in Fig. 10(a)]; however the inferred barrier height from the measurement (filled symbols) shows the opposite trend. This occurs because some of the charge carriers contribute to filling the interface trap states instead of uncovering charge in the semiconductor space-charge region and the details of the interface charge and molecular dielectric layer modulate the potential profile through the device. In addition to introducing significant error in the inferred Φ_B, the presence of high surface-state densities causes a reduction in the apparent doping density from the experimental curves [Fig. 10(b)]. For clarity, molecular dipoles are not included in this calculation; however the observed trends are applicable to dipolar molecular layers as well. The doping densities inferred from the measured *CV* characteristics are in reasonable agreement with the nominal wafer doping density. Based on Fig. 10, this implies that the surface state densities are less than 10^{12} cm^{-2}; therefore the measured Schottky barrier heights from the capacitance measurements are physically reasonable.

IV. DISCUSSION

When dipolar molecular layers are introduced into a metal-semiconductor structure, they can modulate device properties by influencing the surface-state density, as well as through electrostatic effects. By comparing the measured *CV* results with simulations, it is possible to infer which physical effects are responsible for device behavior. The experimentally determined doping densities are in reasonably good agreement with the nominal wafer doping density for all samples. If high surface state densities were present, the apparent doping density would be lower. This indicates that trends in the measured Schottky barrier heights can be attributed to changes in Si surface potential as the surface state densities in these devices are insufficient to influence the measurement. In addition, current-voltage (*IV*) measurements on devices fabricated using the same methods exhibit ideality factors near 1, indicating that the devices have low surface state densities.[32] Some prior studies of MMS diodes have shown ideality factors much greater than 1, indicating that large surface state densities or other physical processes are necessary to describe the devices.[33,34]

Screening effects due to the metal electrode greatly influence the device electrostatics, and the effects are very sensitive to details of the top contact geometry and composition.[13,14,35] Comparisons of the theoretical predictions and the experimental results from *CV* measurements are shown in Fig. 11. For both top contact spacings, the data show a linear relationship indicating that the calculated and

experimental trends are qualitatively similar. From a linear fit, the theoretical prediction for 2 Å top spacing has a slope of 0.3, whereas the 3 Å top spacing calculation has a slope of 0.1. The experimental results are more consistent with the calculations for devices with fairly intimate contact between the metal and the molecular headgroup, indicating that significant screening of molecular charge takes place. Surface potential modulation of Si with the same molecular modifiers has been studied previously using photovoltage measurements. The as-deposited molecular layers were found to induce surface potential changes of −25 mV/D when the sample was in an electrolyte environment.[36] Collectively, these observations suggest that molecular dipole-induced surface potential modulation is present; however there is partial screening of this effect due to the presence of the gold contact.

As shown in Fig. 10, the presence of high surface-state densities in such devices can affect both the Schottky barrier height and the validity of the barrier height inferred from capacitance measurements. In MMS devices, the molecular layers generally cannot occupy every site on the semiconductor surface for steric reasons; however the surfaces still show remarkable chemical stability.[37] It is possible that additional electronic states exist at the surface due to the remaining hydrogen-terminated surface sites, oxidation of the silicon surface, and defects in the molecular monolayer. Prior spectroscopic studies of these molecular layers indicate that some Si backbond oxidation occurs and the extent of this oxidation is dependent on the molecular substituent.[18,20] The good agreement between the nominal doping density and the experimentally determined doping density as well as the low ideality factors from the *IV* measurements suggest that the electronic surface state densities in these devices are quite low. It appears that the molecular layers have a stabilizing effect on the surface even though they do not passivate every dangling bond. Low surface state densities ranging from 3×10^{9} to 3×10^{11} cm^{-2} have been reported for alkyl-terminated Si ⟨111⟩ surfaces.[38,39] Several other mechanisms for charge storage within the junction can occur, including molecular[40] and metal[41] effects. These effects, if interpreted incorrectly, can lead to errors in the inferred barrier height from capacitance measurements. The determination of physically meaningful Schottky barrier heights from capacitance measurements requires that the devices have low interface state densities, as is the case in this study, or that appropriate analysis is used to correct for this effect.

The findings and methods presented here can be generalized to a variety of organic molecule-functionalized semiconductor surfaces. In particular, sensing of chemical and biological materials using charge-based solid-state approaches is a topic of great current interest. Although a variety of devices have been experimentally demonstrated, the observed changes in semiconductor surface potential have generally been small. The importance of top contact screening effects, either due to a metal or ions in solution, can explain the relatively modest responses realized to date.[42] The methodology presented here for calculating expected changes in semiconductor surface potential can be applied to this class of problems through the use of appropriate molecular charge densities and top metal contacts or counterions. The results suggest that improved electrostatic control over semiconductor surfaces in MMS devices can be achieved by reducing the interaction between the molecular charge and the metal, perhaps by adding a very thin insulating layer or insulating molecular functional group adjacent to the metal.

V. CONCLUSION

A series of gold-molecule-silicon diodes with dipolar molecular layers have been fabricated and characterized using *CV* measurements. Complementary calculations were performed to determine the effects of molecular charge density, Si surface states, and metal-molecule interaction effects on the overall device capacitive properties. By correlating experimental results with calculations, it was determined that Si surface state densities in these structures are sufficiently low that they do not affect the capacitance characterization. Experimentally observed trends in Schottky barrier height were consistent with calculated trends in Si surface potential, indicating that the charge distribution within the molecule is modulating the device characteristics. The modest magnitude of this effect is consistent with calculations in which the gold top contact is relatively close to the top atom of the molecular layer, indicating that screening of molecular charge due to the top metal contact is an important effect in such devices.

ACKNOWLEDGMENTS

The authors would like to thank Avik Ghosh and Smitha Vasudevan for helpful discussion. This work is supported by NSF (Grant No. ECE0506802), NASA-URETI (Grant No. NCC3-1363), DoD MURI program, and the Office of Naval Research. A.S. was supported by a NSF Graduate Research Fellowship.

[1] D. K. Aswal, S. Lenfant, D. Guerin, J. V. Yakhmi, and D. Vuillaume, Anal. Chim. Acta **568**, 84 (2006).
[2] H. Akkerman and B. de Boer, J. Phys.: Condens. Matter **20**, 013001 (2008).
[3] C. Joachim, J. K. Gimzewski, and A. Aviram, Nature (London) **408**, 541 (2000).
[4] D. Cahen, A. Kahn, and E. Umbach, Mater. Today **8**, 32 (2005).
[5] A. Vilan, A. Shanzer, and D. Cahen, Nature (London) **404**, 166 (2000).
[6] Y. Selzer and D. Cahen, Adv. Mater. (Weinheim, Ger.) **13**, 508 (2001).
[7] D. G. Wu, J. Ghabboun, J. M. L. Martin, and D. Cahen, J. Phys. Chem. B **105**, 12011 (2001).
[8] A. Vilan, J. Ghabboun, and D. Cahen, J. Phys. Chem. B **107**, 6360 (2003).
[9] A. Scott, D. B. Janes, C. Risko, and M. A. Ratner, Appl. Phys. Lett. **91**, 033508 (2007).
[10] S. Lodha, P. Carpenter, and D. B. Janes, J. Appl. Phys. **99**, 024510 (2006).
[11] G. Ashkenasy, D. Cahen, R. Cohen, A. Shanzer, and A. Vilan, Acc. Chem. Res. **35**, 121 (2002).
[12] A. Salomon, T. Boecking, O. Seitz, T. Markus, F. Amy, C. Chan, W. Zhao, D. Cahen, and A. Kahn, Adv. Mater. (Weinheim, Ger.) **19**, 445 (2007).
[13] H. Haick, M. Ambrico, T. Ligonzo, R. T. Tung, and D. Cahen, J. Am. Chem. Soc. **128**, 6854 (2006).
[14] H. Haick, O. Niitsoo, J. Ghabboun, and D. Cahen, J. Phys. Chem. C **111**, 2318 (2007).
[15] H. Haick, J. Ghabboun, O. Niitsoo, H. Cohen, D. Cahen, A. Vilan, J. Hwang, A. Wan, F. Amy, and A. Kahn, J. Phys. Chem. B **109**, 9622 (2005).
[16] A. Salomon, T. Boecking, C. K. Chan, F. Amy, O. Gershewitz, D. Cahen, and A. Kahn, Phys. Rev. Lett. **95**, 266807 (2005).
[17] O. Seitz, T. Bocking, A. Salomon, J. J. Gooding, and D. Cahen, Langmuir **22**, 6915 (2006).

[18]A. Scott and D. B. Janes, J. Appl. Phys. **105**, 073512 (2009).
[19]R. M. Metzger, T. Xu, and I. R. Peterson, J. Phys. Chem. B **105**, 7280 (2001).
[20]A. Scott and D. B. Janes, J. Phys. Chem. C **112**, 14021 (2008).
[21]D. K. Schroder, *Semiconductor Material and Device Characterization*, 2nd ed. (Wiley, New York, 1998).
[22]S. M. Sze, *Physics of Semiconductor Devices*, 2nd ed. (Wiley-Interscience, USA, 1981).
[23]A. D. Becke, Phys. Rev. A **38**, 3098 (1988).
[24]A. D. Becke, J. Chem. Phys. **98**, 5648 (1993).
[25]C. Lee, W. Yang, and R. G. Parr, Phys. Rev. B **37**, 785 (1988).
[26]J. Kong, C. A. White, A. I. Krylov, D. Sherrill, R. D. Adamson, T. R. Furlani, M. S. Lee, A. M. Lee, S. R. Gwaltney, T. R. Adams, C. Ochsenfeld, A. T. B. Gilbert, G. S. Kedziora, V. A. Rassolov, D. R. Maurice, N. Nair, Y. Shao, N. A. Besley, P. E. Maslen, J. P. Dombroski, H. Daschel, W. Zhang, P. P. Korambath, J. Baker, E. F. C. Byrd, T. Van Voorhis, M. Oumi, S. Hirata, C.-P. Hsu, N. Ishikawa, J. Florian, A. Warshel, B. G. Johnson, P. M. W. Gill, M. Head-Gordon, and J. A. Pople, J. Comput. Chem. **21**, 1532 (2000).
[27]P. Allongue, C. H. de Villeneuve, J. Pinson, F. Ozanam, J. N. Chazalviel, and X. Wallart, Electrochim. Acta **43**, 2791 (1998).
[28]L. Segev, A. Salomon, A. Natan, D. Cahen, L. Kronik, F. Amy, C. K. Chan, and A. Kahn, Phys. Rev. B **74**, 165323 (2006).
[29]D. Deutsch, A. Natan, Y. Shapira, and L. Kronik, J. Am. Chem. Soc. **129**, 2989 (2007).
[30]A. Natan, L. Kronik, and Y. Shapira, Appl. Surf. Sci. **252**, 7608 (2006).
[31]A. Natan, Y. Zidon, Y. Shapira, and L. Kronik, Phys. Rev. B **73**, 193310 (2006).
[32]A. Scott, Ph.D. thesis, Purdue University, 2008.
[33]F. Camacho-Alanis, L. Wu, G. Zangari, and N. Swami, J. Mater. Chem. **18**, 5459 (2008).
[34]M. E. Aydin and F. Yakuphanoglu, J. Phys. Chem. Solids **68**, 1770 (2007).
[35]O. Gershevitz, C. N. Sukenik, J. Ghabbound, and D. Cahen, J. Am. Chem. Soc. **125**, 4730 (2003).
[36]P. Hartig, T. Dittrich, and J. Rappich, J. Electroanal. Chem. **524-525**, 120 (2002).
[37]J. M. Buriak, Chem. Commun. (Cambridge) **1999**, 1051.
[38]W. J. Royea, A. Juang, and N. S. Lewis, Appl. Phys. Lett. **77**, 1988 (2000).
[39]S. Kar, C. Miramond, and D. Vuillaume, Appl. Phys. Lett. **78**, 1288 (2001).
[40]A. Mahapatro, J. Ying, T. Ren, and D. B. Janes, Nano Lett. **8**, 2131 (2008).
[41]L. H. Yu, C. D. Zangmeister, and J. G. Kushmerick, Nano Lett. **6**, 2515 (2006).
[42]P. R. Nair and M. A. Alam, Nano Lett. **8**, 1281 (2008).